PHYSICAL REVIEW B VOLUME 41, NUMBER 4 1 FEBRUARY 1990

Spectral function of the Anderson model: A quantum Monte Carlo calculation

Ofer Biham, Mark Jarrell, and C. Jayaprakash
Department of Physics, The Ohio State University, Columbus, Ohio 43210
(Received 18 August 1989)

We have obtained the spectral function of the asymmetric Anderson model at low temperature through analytic continuation of quantum Monte Carlo data. While not quantitatively exact, the qualitative features of the spectral function clearly allow us to distinguish between the local-moment, mixed-valent, and empty-orbital regimes. We show how the spectral function changes as a function of particle-hole asymmetry and the Coulomb potential U.

In this paper we present the first results for the spectral function of the asymmetric Anderson model of magnetic impurities in a metallic host obtained by directly analytically continuing Monte Carlo data.[1,2] We use a method recently developed by two of us.[1] Unlike previous methods used for the Anderson model,[3] this method is relatively insensitive to statistical noise in the Monte Carlo data. Given the limitations of our procedure and of the Monte Carlo data, we can obtain the qualitative features of the spectral function which allow one to distinguish between the local-moment, mixed-valent, and empty-orbital regimes.

All the thermodynamic properties, as well as the t matrix can be derived from the spectral function of the Anderson model. Experimentally, the spectral function can be measured through different measurements of the density of states [i.e., bremsstrahlung isochromat spectroscopy (BIS) above the Fermi level, and x-ray photoemission below]. Theoretically, the spectral function can be obtained through perturbation expansion in U,[4] or a large degeneracy $(1/N)$ expansion.[5] However, perturbation theory is limited to small values of U, while $1/N$ expansions are limited to the case of both large degeneracy and asymmetry where the impurity is never multiply occupied.

Here we present results from a direct continuation of quantum Monte Carlo data. While our results are only qualitatively correct, limited by resolution and noise in the data, they nevertheless are pertinent for large values of U, the nondegenerate case (spin $\frac{1}{2}$), and all the way from the symmetric to the asymmetric regime.

Using quantum Monte Carlo data, we generate the imaginary-time single-particle Anderson impurity Green's function. We Fourier-transform it to obtain the Matsubara frequency Green's function $G(i\nu_n)$. The problem is to analytically continue $G(i\nu_n)$ in order to obtain the spectral function $A(\omega)$ for real frequencies.

Our analytic continuation technique is based upon the spectral representation of the Green's function,

$$G(i\nu_n)=\int_{-\infty}^{\infty}\frac{A(\omega)}{i\nu_n-\omega}d\omega\,. \tag{1}$$

Here, $\nu_n=(2n+1)\pi T$ and $A(\omega)$ is the corresponding spectral function normalized to 1. We discretize the spectral function by expanding it as a series of δ functions, $A(\omega)=\sum_{m=-\infty}^{\infty}A_m\delta(\omega-\omega_m)$, and choose the real frequencies on a regular grid of spacing $\Delta\omega$. Using this representation of A, Eq. (1) becomes

$$G(i\nu_n)=-\sum_{m=-\infty}^{\infty}\frac{(\omega_m+i\nu_n)A_m}{\omega_m^2+\nu_n^2}\,, \qquad n=0,\pm1,\pm2,\ldots\,. \tag{2}$$

In practice, the Monte Carlo calculation provides us with a finite number of points $G(i\nu_n)$, $n=-N,\ldots,0,\ldots,N-1$. Since the real part of $G(i\nu_n)$ is an even function while its imaginary part is odd we can decompose (2) into a set of N-independent equations for the real part and N for the imaginary part of $G(i\nu_n)$. In order to solve these equations we consider $\{A_p\}$ as a set of dynamical variables evolving in an artificial time t.[1] We then integrate[6]

$$-\frac{\partial A_n}{\partial t}=\mathrm{Im}G(i\nu_n)+\sum_{m=-N}^{N-1}\frac{A_m\nu_n}{\omega_m^2+\nu_n^2}+B(\{A_p\})\,,\quad n=0,\ldots,N-1\,, \tag{3}$$

$$-\frac{\partial A_{-(n+1)}}{\partial t}=\left[\mathrm{Re}G(i\nu_n)+\sum_{m=-N}^{N-1}\frac{A_m\omega_m}{\omega_m^2+\nu_n^2}\right]\mathrm{sgn}(\omega_n)+B(\{A_p\})\,,\quad n=0,\ldots,N-1\,, \tag{4}$$

with

$$B(\{A_p\})=4C_s\left[\sum_{m=-N}^{N-1}A_m-1\right]^3+2C_G(A_{n-2}-44_{n-1}+6A_n-4A_{n+1}+A_{n+2})/(\Delta\omega)^4\,, \tag{5}$$

from $t=0$ until they converge to a fixed point, where $\partial A_n/\partial t=0$. The resulting set $\{A_p\}$ defines the desired spectral function.

The term $B(\{A_p\})$ imposes two physical constraints. Its first part is introduced in order to impose the sum rule

$\int_{-\infty}^{\infty} A(\omega)d\omega = 1$, while the second part tends to suppress spurious fluctuations which result from the singular nature of the linear system and noise in the data. In addition, we do not allow any of the set $\{A_p\}$ to become negative, in the course of the evolution under Eqs. (3) and (4), since $A(\omega)$ is positive definite.

We generate the Green's function on Matsubara frequencies using a quantum Monte Carlo algorithm similar to that developed by Hirsch and Fye.[7] In this simulation the problem is cast into a discrete path-integral formalism in imaginary time, τ_l. The action is evaluated on a grid of L time slices. A discrete Hubbard-Stratonovich transformation, which introduces an Ising field $\sigma(\tau_l)$, is used to make the Hamiltonian quadratic in fermion operators. The fermion degrees of freedom are then integrated out, and one is left with an effective action, which is a function of the Ising field. The Monte Carlo algorithm is constructed to provide an importance sampling of $\sigma(\tau_l)$.

In Ref. 1 we found that our resolution was limited by the imaginary time step $\Delta\tau$. To partially alleviate these problems, we have developed a novel modification of the algorithm: We chose to make the imaginary time grid inhomogeneous, resolving the time slices close to 0 or β a few times finer than those close to $\beta/2$. Since the Green's function $G(\tau)$ is measured at each time difference $\tau-\tau'$, this allowed us to measure $G(\tau)$ on a much finer grid. This gave us more resolution, at the cost of increasing the variance of each measured value. Typically, with $L=160$, we would resolve the first and last 14 time slices 3 times finer than those in the middle, resulting in 312 different time differences. These data were Fourier-transformed to the first N Matsubara frequencies and then analytically continued using the procedure outlined earlier.

The Anderson model, in the limit of infinite metallic bandwidth,

$$H=\sum_{k,\sigma}\epsilon_k C_{k,\sigma}^{\dagger}C_{k,\sigma}+V\sum_{k,\sigma}(C_{k,\sigma}^{\dagger}d_{\sigma}+d_{\sigma}^{\dagger}C_{k,\sigma}) +\epsilon_d\sum_{\sigma}n_{d\sigma}+Un_{d\uparrow}n_{d\downarrow} \tag{6}$$

is characterized by a hybridization width $\Delta=\pi N(0)V^2$ [where V is the hybridization matrix element, and $N(0)$ is the density of states at the Fermi surface], an on-site repulsion U, and a Kondo temperature,[8,9]

$$T_K=0.364(2\Delta U/\pi)^{1/2}e^{\pi\epsilon_d(\epsilon_d+U)/2\Delta U}, \tag{7}$$

obtained from perturbation theory. We present results for the spectral density at low temperature (low compared to the appropriate characteristic energy scale) as one varies ϵ_d from the symmetric regime ($\epsilon_d=-U/2$) to the extreme asymmetric values. An important rigorous result, due to Langreth,[10] is the Friedel sum rule

$$A(\omega=0,T=0)=\frac{\sin^2(\pi\langle n_{d\sigma}\rangle)}{\pi\Delta}, \tag{8}$$

where $\langle n_{d\sigma}\rangle$ is the occupancy of the orbital with spin σ. There are three low-temperature regimes: (i) the local moment regime in which, at low temperatures, the moment is quenched by the Kondo effect with a characteristic energy scale T_K, this occurs for $\epsilon_d<-\Delta$ and $\langle n_{d\sigma}\rangle\approx\frac{1}{2}$; (ii) the mixed-valent regime, characterized by an energy scale Δ, where the ground state is a singlet with $0.2<\langle n_{d\sigma}\rangle<0.4$; and (iii) the empty-orbital regime which occurs for $\epsilon_d\gg\Delta$.

We first present results for the symmetric Anderson model ($\epsilon_d=-U/2$), as a function of the Coulomb potential U. In the symmetric regime we find $\langle n_{d\sigma}\rangle=0.5$ as expected. In the $U=0$ limit (resonant level model) $A(\omega)$ is a Lorentzian of height $1/(\pi\Delta)$ and half-width Δ. Our result for $U=0$ is given in Fig. 1. The peak has the right height and width, however, the tail is not reproduced as a result of the cutoff imposed by the finite number of input data points. The weight associated with the tail was shifted inwards forming two side branches. For finite U the spectral function has the typical three-peak structure (solid line in Fig. 1). There are two broad peaks with half-width of order Δ, whose positions are given approximately by ϵ_d and ϵ_d+U, corresponding to $d^0\rightarrow d^1$ and $d^1\rightarrow d^2$ transitions, respectively. At $\omega=0$ we find the Abrikosov-Suhl resonance which is expected to have a width of order T_K at zero temperature. The actual result is considerably broader for two reasons. Primarily it is due to the limited resolution of the analytic continuation method. In addition, the simulations were performed at temperatures $T\approx T_K$, and hence there is non-negligible thermal broadening.[5] The latter also accounts for the fact that the peak is somewhat lower than expected from the Friedel sum rule. We have found that in simulations in which $T\approx 0.25T_K$, the Friedel sum rule is satisfied to better than 8% accuracy.

As we move away from the symmetric regime, for $|\epsilon_d|<(U-\Delta)/2$, the system continues to exhibit a local moment (at high temperatures) that is quenched for $T<T_K$, the spectral function changes slightly from Fig. 1: The central Abrikosov-Suhl peak is a bit broader, consistent with the fact that T_K has increased, and is also dis-

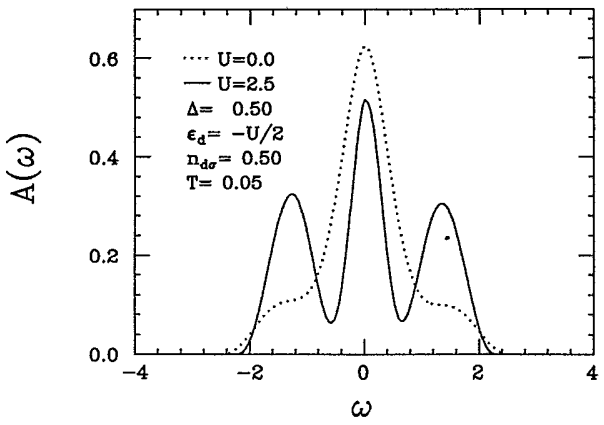

FIG. 1. The spectral density of the symmetric Anderson model (at $\Delta=0.5$) as a function of the Coulomb potential U. For $U=0$ (dotted line) our results are in agreement with the exact $A(\omega)$ which is a Lorentzian of height $1/(\pi\Delta)$ and half-width Δ (see text). For $U=2.5$ (solid line), where $T_k=0.05$ we find two side peaks at $\omega=\epsilon_d$ and $\omega=\epsilon_d+U$, while the central peak becomes narrower and does not retain a Lorentzian shape (Ref. 5).

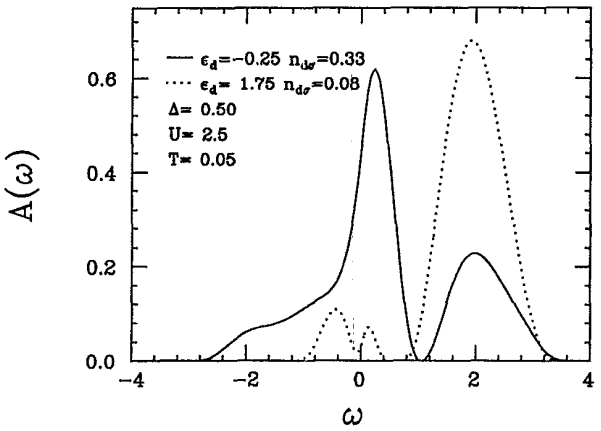

FIG. 2. The spectral density of the Anderson model when $U=2.5$ and $\Delta=0.5$ for two values of ϵ_d. For $\epsilon_d=-0.25$ (solid line) the shape is typical to the mixed-valent regime. Here the lower peak merges with the central peak, while the upper peak retains its identity and the expected position ϵ_d+U. For $\epsilon_d=1.75$ (dotted line) we enter the empty-orbital regime in which there is a single peak whose position and height are given accurately by the Hartree result [position $\approx \epsilon_d+U\langle n_{d\sigma}\rangle$ and height $1/(\pi\Delta)$]. The small wiggles at low frequencies seem to be an artifact of the method of analytic continuation, however, the Friedel sum rule is still satisfied.

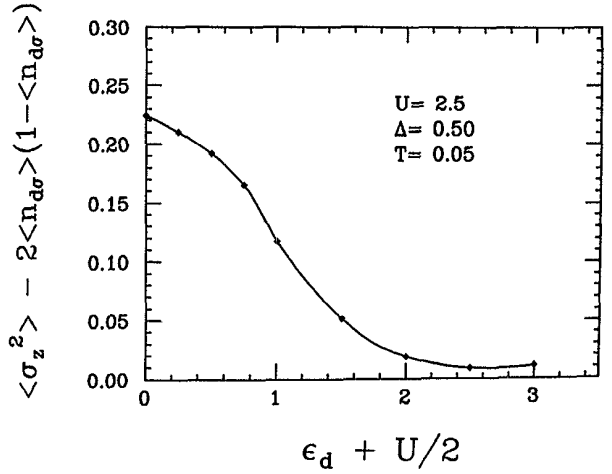

FIG. 3. The subtracted moment $\langle\sigma_z^2\rangle-2\langle n_{d\sigma}\rangle(1-\langle n_{d\sigma}\rangle)$ vs ϵ_d. This quantity is finite when a local moment is present, independent of Kondo screening. In the local-moment regime $(0.0<\epsilon_d+U/2<0.75)$, this quantity falls slowly with $\epsilon_d+U/2$. In the mixed-valent regime, it falls quickly. In the empty-orbital regime it is essentially zero, indicating no local moment.

placed from zero. The two broad peaks show the expected asymmetry in position, with the upper peak rising in height and position. This distinct three-peak structure persists until $\langle n_{d\sigma}\rangle\approx 0.4$.

As ϵ_d increases further we enter the mixed-valent regime. From the perturbative scaling analysis,[8] and the nonperturbative renormalization group,[9] it is known that the singlet state is renormalized downward in energy more than the triplet. Typically this regime is discussed in the limit where U is much larger then ϵ_d and Δ.[11] We explore the values $|\epsilon_d|>(U-\Delta)/2$ with U fixed. As $\langle n_{d\sigma}\rangle$ decreases below 0.4, the lower peak merges with the central peak as shown in Fig. 2. The upper peak ($d^1\rightarrow d^2$ transition) retains its identity and is at the expected position (ϵ_d+U). Its spectral weight is smaller, since the ground state now has less projection onto the singly occupied state. In this regime, therefore, the spectral function exhibits two broad peaks (of half-width Δ). The precise shape of the lower peak, which is more pronounced, is quite sensitive to the values of ϵ_d. We find that this regime occurs for $\epsilon_d\lesssim 2\Delta$.

Finally, we increase ϵ_d sufficiently to reach the empty-orbital regime where there is a single peak (Fig. 2) whose position and height are given accurately by the Hartree result [position $\approx\epsilon_d+U\langle n_{d\sigma}\rangle$ and height $1/(\pi\Delta)$]. The small wiggles in the low-frequency structure in Fig. 2 seem to be an artifact of the method of analytic continuation. We do note, however, that the low-frequency structure does satisfy the Friedel sum rule (as expected since the characteristic energy scale in this regime is Δ).

We have also found it useful to monitor $\langle\sigma_z^2\rangle=\langle(n_{d\uparrow}-n_{d\downarrow})^2\rangle$ as a measure of the local moment on the impurity. In the uncorrelated regime ($U=0$ or $\epsilon_d\gg U$), $\langle\sigma_z^2\rangle=2\langle n_{d\sigma}\rangle(1-\langle n_{d\sigma}\rangle)$. In Fig. 3 we plot $\langle\sigma_z^2\rangle-2\langle n_{d\sigma}\rangle\times(1-\langle n_{d\sigma}\rangle)$ vs ϵ_d. This quantity is finite when a local moment is present, independent of Kondo screening. In the symmetric case $\langle\sigma_z^2\rangle-2\langle n_{d\sigma}\rangle(1-\langle n_{d\sigma}\rangle)=0.5$ in the limit $U\rightarrow\infty$. In the local-moment regime $(0<\epsilon_d+U/2<0.75)$, this quantity falls slowly with $\epsilon_d+U/2$. In the mixed-valent regime $(0.75<\epsilon_d+U/2<2.0)$, it falls quickly. In the empty-orbital regime $(\epsilon_d+U/2>2.0)$ it is essentially zero, indicating no local moment.

In summary, we have presented the first results for the low-temperature behavior of the spectral density function of the Anderson model obtained by analytic continuation of quantum Monte Carlo data. We have shown how the spectral function changes as a function of particle-hole asymmetry and the Coulomb potential U. By varying these parameters we were able to distinguish between the local-moment, mixed-valent, and empty-orbital regimes. All our calculations were done for a fixed temperature $T=0.05$. Since the resolution of the analytic continuation method becomes worse for higher temperatures we could not perform a systematic study as a function of temperature.

We are pleased to acknowledge useful conversations with D. L. Cox, D. Sullivan, W. Wenzel, and J. W. Wilkins. One of us (C.J.) thanks F. D. M. Haldane for stimulating discussions on this subject many years ago. This work was supported in part by the U.S. Department of Energy–Basic Energy Science, Division of Materials Research, National Science Foundation Grant No. NSF-DMR8451911, and the Ohio Supercomputer Center.

[1]M. Jarrell and O. Biham, Phys. Rev. Lett. **63**, 2504 (1989).

[2]S. R. White, D. J. Scalapino, R. L. Sugar, and N. E. Bickers, Phys. Rev. Lett. **63**, 1523 (1989).

[3]J. Hirsch, in *Quantum Monte Carlo Methods,* edited by M. Suzuki, Springer Series in Solid State Sciences Vol. 74 (Springer-Verlag, Heidelberg, 1987).

[4]B. Horvatic, D. Sokcevic, and V. Zlatic, Phys. Rev. B **36**, 675 (1987).

[5]N. E. Bickers, D. L. Cox, and J. W. Wilkins, Phys. Rev. B **36**, 2036 (1987).

[6]This identification of $\partial A_n/\partial t$ with the right-hand side of the equation is not unique. For example, one may exchange the right-hand sides of the two equations, and still converge to the same final result.

[7]J. E. Hirsch and R. M. Fye, Phys. Rev. Lett. **56**, 2521 (1986).

[8]F. D. M. Haldane, Phys. Rev. Lett. **40**, 416 (1978).

[9]H. R. Krishna-murthy, J. W. Wilkins, and K. G. Wilson, Phys. Rev. B **21**, 1003 (1979).

[10]D. C. Langreth, Phys. Rev. **150**, 516 (1966).

[11]A. M. Tsvelick and P. B. Weigmann, Adv. Phys. **32**, 453 (1983).